

Article

WRKY22 Transcription Factor from *Iris laevigata* Regulates Flowering Time and Resistance to Salt and Drought

Lijuan Fan, Zhaoqian Niu, Gongfa Shi, Ziyi Song, Qianqian Yang, Sheng Zhou and Ling Wang *

College of Landscape Architecture, Northeast Forestry University, Harbin 150040, China; flj@nefu.edu.cn (L.F.); niuzhaoqian@nefu.edu.cn (Z.N.); sumu@nefu.edu.cn (G.S.); 2000lhszy@nefu.edu.cn (Z.S.); 16650601598@nefu.edu.cn (Q.Y.); liuguilin90@126.com (S.Z.)

* Correspondence: wanglinghlj@nefu.edu.cn

Abstract: *Iris laevigata* Fisch. is an excellent ornamental plant in cold regions due to its unique ornamental ability and strong cold resistance. However, the flowering period of the population is only about 20 days, greatly limiting its potential uses in landscaping and the cutting flower industry. In addition, *I. laevigata* is often challenged with various abiotic stresses including high salinity and drought in its native habitats. Thus, breeding novel cultivars with delayed flowering time and higher resistance to abiotic stress is of high importance. In this study, we utilized sequencing data from the *I. laevigata* transcriptome to identify WRKYs and characterized *IIWRKY22*, a key transcription factor that modulates flowering time and abiotic stress responses. *IIWRKY22* is induced by salt and drought stress. We cloned *IIWRKY22* and found that it is a Group IIe WRKY localized in the nucleus. Overexpressing *IIWRKY22* in *Arabidopsis thaliana* (L.) Heynh. and *Nicotiana tabacum* L. resulted in a delayed flowering time in the transgenic plants. We created transgenic *N. tabacum* overexpressing *IIWRKY22*, which showed significantly improved resistance to both salt and drought compared to the control plants. Thus, our study revealed a unique dual function of *IIWRKY22*, an excellent candidate gene for breeding novel *Iris* cultivars of desirable traits.

Keywords: *Iris*; WRKY transcription factor; flowering time regulation; salt stress; drought stress



Citation: Fan, L.; Niu, Z.; Shi, G.; Song, Z.; Yang, Q.; Zhou, S.; Wang, L. WRKY22 Transcription Factor from *Iris laevigata* Regulates Flowering Time and Resistance to Salt and Drought. *Plants* **2024**, *13*, 1191. <https://doi.org/10.3390/plants13091191>

Academic Editor: Vladimir V. Kuznetsov

Received: 20 March 2024

Revised: 17 April 2024

Accepted: 23 April 2024

Published: 25 April 2024



Copyright: © 2024 by the authors. Licensee MDPI, Basel, Switzerland. This article is an open access article distributed under the terms and conditions of the Creative Commons Attribution (CC BY) license (<https://creativecommons.org/licenses/by/4.0/>).

1. Introduction

A key event in the life cycle of angiosperms is the formation of flowers, which marks the transitions of plants from vegetative growth to reproductive growth [1]. It not only directly affects the growth, development, and yield of crop plants but also has a great impact on horticultural plants as the flower is the most important ornamental part in landscaping [2]. Flowering is controlled by a very large and fine-tuned regulatory network, which integrates various exogenous and endogenous factors to determine the most appropriate flowering time [3–5]. In response to various environmental factors that influence flowering, plants have developed multiple pathways with multiple transcription factors (TFs) for the transition to flowering. The critical roles of TFs in flowering have been extensively studied [6]. Some of the most important proteins in flowering pathways are TFs or transcriptional regulators including CONSTANS (CO) in the photoperiod pathway and flowering locus C (FLC), a MADS-box TFs that represses flowering. Major flowering pathways include the photoperiod pathway, which involves the de-repression of cycling of factors (CDF) on CO and flowering locus T (FT), as well as the vernalization, temperature, and autonomous pathways, which involve the de-repression of FLC on FT. Additionally, the GA pathway involves the de-repression of suppressor of overexpression of CONSTANS1 (SOC1) through the degradation of DELLA proteins [7].

On the other hand, various environmental stresses such as high temperature, cold, salinity, and drought can inhibit the metabolism and growth in plants [8]. High salinity and drought are two main abiotic stresses that affect plant growth and development and even cause death [9]. Salt stress causes ion imbalance, osmotic stress, and secondary oxidative

stress, resulting in impaired photosynthetic capacity and intracellular nutrient metabolism imbalance and ultimately affecting plant development and yield. Under high salinity, ions from the soil accumulate in the cytoplasm and thus disrupt the osmotic regulation. Ion imbalance can last a few days or even weeks in tender parts of the plants such as the bud [10]. It further induces secondary oxidative stress, leading to the inhibition of photosynthesis and metabolism and ultimately a deduction in plant yield [11]. Similar to high salinity, drought causes osmotic stress and secondary stress including oxidative stress, damage to cellular components, and metabolic dysfunction [10]. Therefore, drought and salt stress have certain overlapping signals [12]. In addition, evolution and adaptation equip plants to quickly sense stress signals via TFs such as WRKYs and gene regulatory networks [13,14]. WRKY exhibits a rapid response to adverse environments and plays a crucial role in enhancing the tolerance of various plants to abiotic stress [4]. TFs play a critical role in the responses to abiotic stresses by activating or inhibiting the expression of target genes, leading to reprogramming in plant metabolism and adaptability to abiotic stress [15]. Thus, there is an increased interest in using TFs to combat environmental stresses in the face of global warming [16,17]. For instance, *HaWRKY22* enhances the drought stress tolerance of *Helianthus annuus* L. [18], while *PsWRKY22* from *Prunus salicina* Lindl. enhances tolerance to both salt and drought stress [19].

Thus, the two seemingly unrelated processes of flowering and response to salt and natural drought stress have one thing in common: both are under tight control of TFs. Interestingly, TFs may regulate multiple independent biological processes because they can interact with distinct sets of substrates. The WRKY family is a good example that controls a diverse range of physiological events via a complex gene network [20,21]. For instance, WRKY regulates plant tolerance to various stresses such as low temperature, salt, high temperature, drought, and flowering by interacting with abscisic acid (ABA), jasmonic acid (JA), and ROS. WRKYs are named after the highly conserved WRKYGQK domain at the N-terminus [22]. The C terminus contains a CX₄-7CX₂₂ or 23HXX/C zinc finger that is important for protein interactions and DNA binding [20,23]. Based on the number of WRKY domains and the type of zinc finger structure, WRKYs are categorized into three groups: group I (two WRKY domains and a C₂H₂-type zinc finger structure), group II (one WRKY domain and a C₂H₂-type zinc finger structure), and group III (one WRKY domain and a C₂HC-type zinc finger structure) [24]. With the advancement of sequencing technologies, WRKYs have been identified on a genome-wide scale in many plant species. For example, there are 74 members in *A. thaliana*, 59 in *Vitis vinifera* L., 127 in *Malus pumila* Mill., 102 in *Oryza sativa* L., and 119 in *Zea mays* L. [25].

I. laevigata is native to northeast China with strong cold resistance and beautiful flowers of unique shape and bright color [26]. Such desirable traits make *I. laevigata* a good candidate for both landscaping and industrial use as a cutting flower. However, the potential is dampened because of the short flowering period with only 2 days for a single flower and 20 days for the population [26]. To stagger the flowering time and prolong the flowering period, it is necessary to find genes that can advance or delay the flowering. *I. laevigata* is also sensitive to abiotic stress [27]. Thus, extending the flowering period and increasing the resistance to salt and drought stress are two central goals in the field of breeding *I. laevigata* of novel properties [28,29]. One prerequisite to achieve these goals is to identify key genes controlling the target traits, which has been propelled tremendously by the advances in transcriptome sequencing [30–32].

However, molecular studies in *I. laevigata* are difficult due to the lack of genome information [26]. Our group pioneered the first transcriptomics studies in the tepals of *I. laevigata*. In this study, we report the identification of 68 WRKYs in *I. laevigata*, which are distributed to the three groups that regulate multiple biological processes. Among them, group II genes primarily participate in defense responses against bacterial and fungal infections, abiotic stress reactions, aging processes, and developmental phenomena [33]. WRKY22, a member of the group II transcription factor family within the WRKY family, has been demonstrated to play a pivotal role in conferring resistance against bacteria [34].

low temperature [35], and abiotic stressors [18,19], as well as governing the regulation of flowering [36]. To promote resistance and flowering regulation of swallow flowers, this study focused on the functional validation of *IIWRKY22*.

We found *IIWRKY22* was significantly up-regulated upon salt and drought stress treatment. Furthermore, we cloned *IIWRKY22* and overexpressed it in *N. tabacum*, resulting in enhanced salt and drought tolerance. Overexpressing *IIWRKY22* in *A. thaliana* and *N. tabacum* led to a delay in flowering, which was accompanied by the dysregulation of many flowering transcription factors including CO and GA-20 oxidase (GA20OX), SOC1, and squamosa promoter binding protein like3 (SPL3). Thus, our data demonstrated that *IIWRKY22* is a negative regulator in flowering and a positive regulator in resistance to salt and drought. In conclusion, *IIWRKY22* is a multifaceted TF that can be tweaked to improve multiple traits. Our findings have the potential to extend the flowering period of *I. laevigata* through the cultivation of late-flowering transgenic plants alongside wild type (WT) plants. Because the transgenic plants have stronger salt tolerance and drought resistance, the overall adaptability of *I. laevigata* will also be improved. Together, our results hold promise for the wider implementation of *I. laevigata* in landscaping projects throughout northeastern China.

2. Materials and Methods

2.1. Plant Materials

I. laevigata was outdoor-planted in the nursery of the School of Landscape Architecture, Northeast Forestry University (126°64' E, 45°72' N, Heilongjiang Province, China).

Seeds of *A. thaliana* (ecotype Columbia) Col-0 were surface-sterilized by immersing them in 75% alcohol (Lircon, Dezhou, China) for 1 min, followed by triple rinsing with sterile water. Seeds were then disinfected in 0.8% NaClO (Xilong Scientific, Beijing, China) for 10 min and rinsed 5 times again. Sterilized seeds were sowed on 1/2 MS (Hope Bio-Technology, Qingdao, China), and vernalized at 4 °C in the dark for 2 days, followed by cultivation at a greenhouse under 16 h/8 h (light/dark) at 20 °C. After 7–9 days, seedlings were transferred into a potting mix (peat soil/vermiculite/perlite of 5/3/2) and allowed to grow for 3 weeks before transformation.

N. tabacum seeds were disinfected with 75% alcohol (Lircon, Dezhou, China) for 1 min, followed by triple rinsing with sterile water. Seeds were then disinfected with 2% NaClO (Xilong Scientific, Beijing, China) for 10 min and rinsed with sterile water 5 times. Seeds were cultured in MS (Hope Bio-Technology, Qingdao, China) at 25 °C, with 14 h/10 h (light/dark). Plants of 4–6 true leaves were used for transformation.

2.2. The Treatment of *I. laevigata* under Salt and Drought Stress

In order to further investigate the involvement of *IIWRKY22* in the responses of *I. laevigata* to salt and drought stresses, 1-year-old *I. laevigata* plants with carefully selected for a 7-day water culture experiment. For the salt treatment, the plants were exposed to a concentration of 300 mM NaCl, while for the drought treatment, they were subjected to a concentration of 20% PEG-6000. The expression level of *IIWRKY22* in the leaves was then measured in real-time at 0, 2, 6, 12, and 24 h.

2.3. Gene Sequence Identification and Phylogenetic Analysis

Putative WRKY sequences were identified from the transcriptome data from the tepals of *I. laevigata* with the online annotation tool from the Beijing Genomics Institute (Beijing, China) (<https://www.bgi.com/home>, accessed on 3 January 2023). We downloaded all *A. thaliana* WRKY sequences from the National Center for Biotechnology Information (NCBI) (<https://www.ncbi.nlm.nih.gov/>, accessed on 3 January 2023). Phylogenetic analysis was conducted in MEGA 5.0 (Version 10.1.8) (<https://phytozome-next.jgi.doe.gov/>, accessed on 3 January 2023) using WRKY sequences from both *I. laevigata* and *A. thaliana*. The open reading frames of these sequences were determined by the ORF Finder tool (<https://www.ncbi.nlm.nih.gov/orffinder/>, accessed on 3 January 2023), and

the conserved domains were identified by the CD Search tool (<https://www.ncbi.nlm.nih.gov/Structure/cdd/wrpsb.cgi>, accessed on 3 January 2023). *WRKY* sequences of different species were obtained by BLAST (<https://blast.ncbi.nlm.nih.gov/Blast.cgi>, accessed on 3 January 2023) at NCBI. Multiple sequence alignment was performed using DNAMAN (Version 5.2.2) (<https://www.lynnon.com/dnaman.html>, accessed on 3 January 2023). Sequence alignment was performed using Clustal W (<http://www.clustal.org/clustal2/>, accessed on 3 January 2023), followed by the construction of a phylogenetic tree using the neighbor-joining (NJ) method with 1000 bootstraps. The resulting tree was then annotated using iTOL (<https://itol.embl.de/>, accessed on 3 January 2023).

2.4. Gene Cloning and Sequence Analysis

Total RNA was extracted from the tepals of *I. laevigata* using a kit (Kangweishiji, Taizhou, China), and the integrity was checked by electrophoresis. First-strand cDNA was synthesized using the Primer Script TM RT kit (TakaRa, Beijing, China). *IIWRKY22* (accession number: ON399552) was cloned using KOD-plus-neo (ToYoBo, Shanghai, China) with primers (Ruibo Kexing, Harbin, China) listed in Table S1. The cloned sequences were inserted into the Cloning vector pEASY[®]-Blunt Zero Cloning Kit (TransGen, Beijing, China) and transformed into *Escherichia coli* DH5 α (WEIDI, Shanghai, China). The pCAMBIA1300: *IIWRKY22-GFP* carrier was constructed for heterologous expression through homologous recombination. Homologous recombination primers (Ruibo Kexing, Harbin, China) listed in Table S1. The pCAMBIA1300 vector were digested with Sall and BamHI, which were then used to create pCAMBIA1300-*IIWRKY22-GFP* using ClonExpressII (Vazyme, Nanjing, China). The recombinant vector was transformed into *E. coli* DH5 α (WEIDI, Shanghai, China) for sequencing. Positive plasmids were transferred into *Agrobacterium tumefaciens* GV3101 (WEIDI, Shanghai, China) for subsequent infection experiments. Bioinformatics analysis of *IIWRKY22* was performed as described [26].

2.5. Subcellular Localization

The online tool Cell-PLoc 2.0 was used to predict subcellular localization (<http://www.csbio.sjtu.edu.cn/bioinf/Cell-PLoc-2/>, accessed on 3 January 2023). The subcellular localization of *WRKY22* was experimentally determined as described [37]. Briefly, bacteria GV3101 (WEIDI, Shanghai, China) harboring pCAMBIA1300: *IIWRKY22-GFP* were cultured to an OD₆₀₀ of 0.6–0.8 and collected. After resuspending in 10 mM MgCl₂ to an OD₆₀₀ of 1.5, acetosyringone (Sinopharm, Beijing, China) was added to a final concentration of 200 μ M. The bacterial solution was activated for 3 h in the dark and then injected to the lower side of *Nicotiana benthamiana* Domin. leaves using a syringe. Expression of the fusion protein *WRKY22-GFP* was visualized under an AN-28L fluorescent microscope (Aonuoguangxu, Shenzhen, China) in the transformed epidermal cells [26].

2.6. Plant Transformation

Transgenic *A. thaliana* plants were created using the flower dip method reported before [38]. Seeds of transformed plants were selected on 1/2 MS medium supplemented with 25 mg/L Hyg (Xilong Scientific, Beijing, China). After 7–9 days, T1 seedlings that survived on the screening medium were transferred to a potting mix of peat soil, vermiculite, and perlite in a ratio of 3:2:1. The plants were then cultured at a temperature of 20 °C with a photoperiod of 16 h/8 h (light/dark). Transgenic plants were then screened by PCR, the primers (Ruibo Kexing, Harbin, China) listed in Table S1. Homozygous lines were obtained by 3 consecutive generations of screening. Three lines exhibiting high expression levels were selected.

Agrobacterium-mediated transformation of *N. tabacum* leaf disk and screening of the resulting transgenic plants were performed according to a previously published method [39].

2.7. Determination of Flowering Phenotypes and Gene Expression

Bolting time and flowering time were recorded of each plant, which were observed and counted daily. The survey criteria for bolting time was the time required from seeding to bud visibility. Flowering time was measured as the time required from sowing to the full opening of the first flower [40–44]. The number of rosette leaves was also recorded. The expression levels of CO, GA20OX, vernalization1 (VRN1), SPL3, flowering control local A (FCA), short vegetative phase (SVP), trehalose-6-phosphate synthase1 (TPS1), SOC1, and FLC in *A. thaliana* seedlings at 7, 10, and 14 days of age were determined using real-time quantitative PCR (RT-qPCR) with the $2^{-\Delta\Delta CT}$ method; the primers (Ruibo Kexing, Harbin, China) are listed in Table S1.

2.8. The Treatment of Transgenic *N. tabacum* Salt and Drought Stress

To ensure the accuracy of the data, we set up 3 repeat groups for each line, with 5 plants in each group. Salt and drought stress tests were performed on *IIWRKY22* overexpressed *N. tabacum* using EV and WT controls. Initially, the plants were cultivated in a potting mix consisting of peat soil, perlite, and vermiculite (3:1:1), and under a photoperiod of 16 h of light followed by 8 h of darkness at 28 °C, for a duration of 30 days. Subsequently, plants with comparable overall health were subjected to salt and drought stress treatments. For the salt treatment, plants were watered with 100 mL of a 300 mM NaCl solution every 2 days. In the case of natural drought, plants were deprived of water. Phenotypic observations and leaf samples were collected at 0, 7, and 14 days after the initiation of the treatments.

2.9. Photosynthetic Parameters in *N. tabacum* under Salt and Drought Stress

A Li-6400 (ecotek, Beijing, China) portable photosynthesis instrument was utilized to quantify various photosynthetic parameters including net photosynthetic rate (Pn), stomatal conductance (Gs), intercellular CO₂ concentration (Ci), and transpiration rate (Tr) from 9:00 AM to 10:00 AM. Three individual plants were randomly selected from each line (OE, EV, and WT), and the third and fourth leaf were used for measurement. The Li-6400 instrument was calibrated before taking measurements, and data was recorded after the reading was stable. Five measurements were taken for each leaf [39]. The chlorophyll (Chl) content was assessed using the acetone extraction method [45,46]. The functional leaves of the same part were selected, and the chlorophyll fluorescence parameters of the leaves were determined by using a PAM-2500 (WALZ, Effeltrich, Germany) portable modulated chlorophyll fluorometer [39].

2.10. Other Physiological Measurements under Salt and Drought Stress *N. tabacum* Plants

Commercially available kits (catalog number G0105F, and the same hereafter) from Grace Biotechnology (Shanghai, China) were used for the quantification of CAT, hydrogen peroxide (G0112F), and O₂⁻ (G0116F). The determination method referred to the instructions of the kit. Malondialdehyde (MDA), superoxide dismutase (SOD) activity, and peroxidase (POD) activity were measured based on a previous study [39]. To prepare the stressed *N. tabacum* leaves, leaf discs with a diameter of 1.5 cm were cut, following the protocol described by Wang [39]; p-Nitro-Blue tetrazolium chloride (NBT) and 3,3'-diaminobenzidine tetrahydrochloride (DAB) staining techniques were employed to assess the concentration of superoxide anion and hydrogen peroxide in the leaves, respectively.

2.11. Reverse Transcription PCR (RT-PCR) and RT-qPCR

We set up 3 repeat groups for each line, with 5 plants in each group. The expression patterns of *IIWRKY22* were measured in various parts of *I. laevigata*, including roots, tubers, and leaves under normal growth conditions. Additionally, the response of *IIWRKY22* in leaves of *I. laevigata* 0, 2, 6, 12, and 24 h after salt and drought stress were measured. Randomly selected T3 lines of *A. thaliana* and *N. tabacum* were used for measuring the expression of *IIWRKY22*. Furthermore, the expression levels of stress response genes (*NtCAT*, *NtHAK1*, *NtPMA4*, *NtPOD*, *NtSOD*, and *NtSOS1*) were measured in *N. tabacum*

leaves under NaCl and drought stress for 0, 7, and 14 days. This analysis was conducted in WT, EV, and 3 overexpressed *IIWRKY22* lines. The method used for total RNA extraction and reverse transcription to cDNA was the same as described above. *IIPP2A*, *ACT2*, and *NtTUBA* served as internal reference genes for *I. laevigata*, *A. thaliana*, and *N. tabacum*, respectively. RT-qPCR was performed using the SYBR Green I method, following the instructions provided by UltraSYBR Mixture (CWBI). The results were calculated as $2^{-\Delta\Delta CT}$; the primers (Ruibo Kexing, Harbin, China) are listed in Table S1.

2.12. Statistical Analysis

Data recording and statistical analysis were conducted using Excel (Version 2021). Statistical analyses were performed using SPSS (version 26). Before performing the analysis of variance, the experimental data were subjected to the Shapiro–Wilk and Levene tests to verify residual normality and homoscedasticity, respectively. We used one-way ANOVA of statistical analysis and Duncan’s test. The data were tested for statistical significance within a confidence interval using the least significant difference method ($p < 0.05$). Plots were generated using Origin (version 2021). Statistical differences between the transgenic and control plants were determined.

3. Results

3.1. Identification of WRKY Genes in *I. laevigata*

We performed transcriptome data mining of *WRKY* sequences in the tepals of *I. laevigata* (unpublished). *WRKY* family were obtained by BLAST and sequence analysis. We found a total of 68 putative members (Figure 1). Phylogenetic analysis of the coded proteins showed that they are distributed to groups I (n = 22), IIa (n = 5), IIb (n = 7), IIc (n = 1), IID (n = 13), IIE (n = 9), and III (n = 11). By contrast, the 59 *WRKY* members in *A. thaliana* showed a different pattern of distribution among the groups: groups I (n = 11), IIa (n = 2), IIb (n = 7), IIc (n = 16), IID (n = 6), IIE (n = 6), and III (n = 11). Given the distinctive roles of each group, this may indicate functional divergence of *WRKY* genes in *I. laevigata*.

3.2. Cloning of *IIWRKY22* and Subcellular Localization

We next cloned *WRKY22* using *I. laevigata* cDNA with PCR. The sequence of *IIWRKY22* was 840 bp. Sequence alignment showed that it contains the highly conserved *WRKYGQK* domain (Figure 2A) and it is most similar to *WRKY22* from *Zingiber officinale* (Figure 2B) with the C2H2 zinc finger [20], a typical feature of the group IIE of the *WRKY* family.

The *IIWRKY22* protein was predicted to be in the nucleus. To verify this *in vivo*, we transiently expressed an *IIWRKY22*-GFP fusion protein in *N. benthamiana* leaves. We found the fusion protein is exclusively expressed in the nucleus of epidermal cells (Figure 2C). Thus, this data supported the prediction and agreed with the putative TF function of *IIWRKY22*.

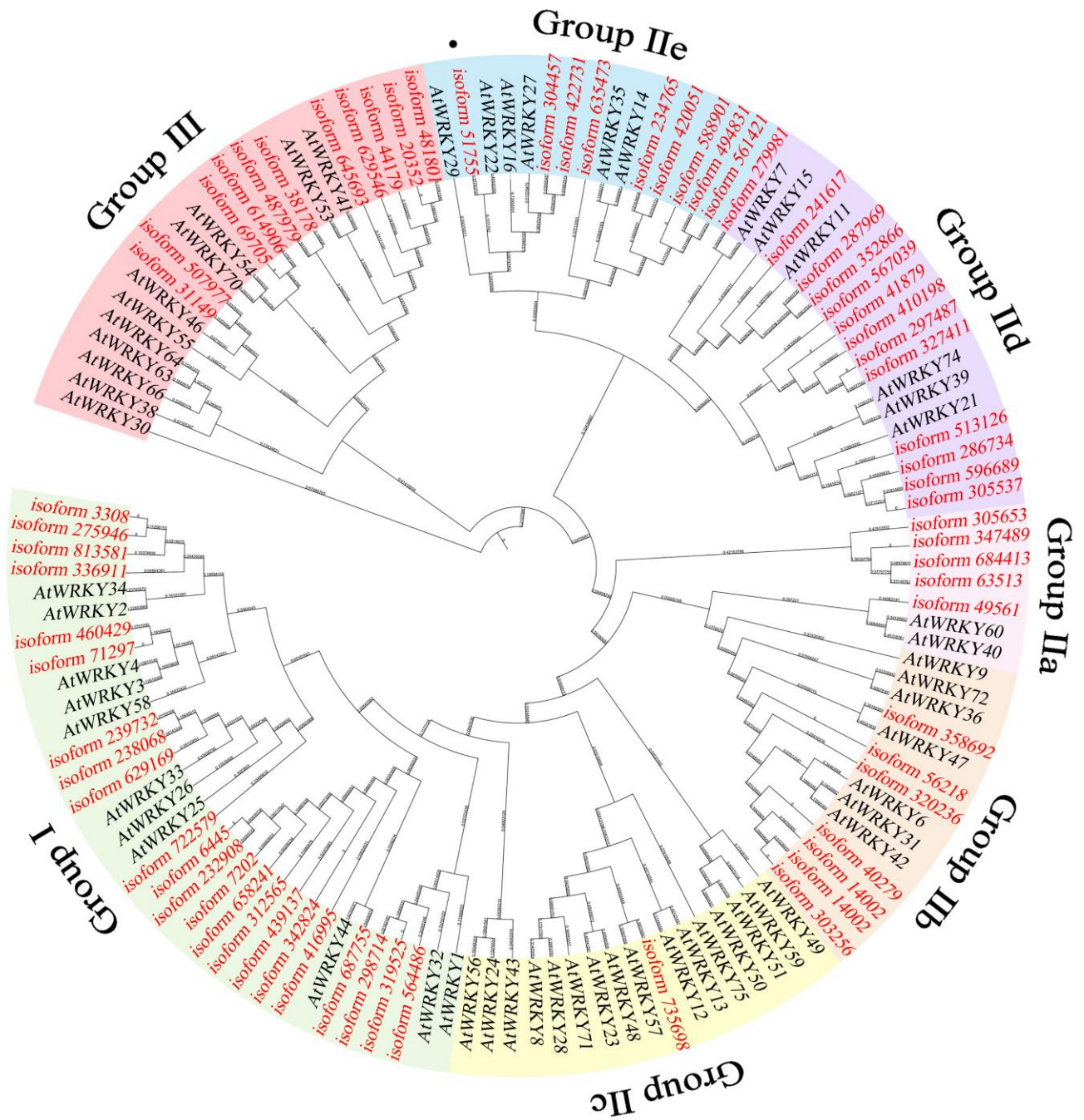


Figure 1. Phylogenetic analysis of WRKYs from *I. laevigata* (in red) and *A. thaliana* (in black). Black dots indicate IIWRKY22 from *I. laevigata*.

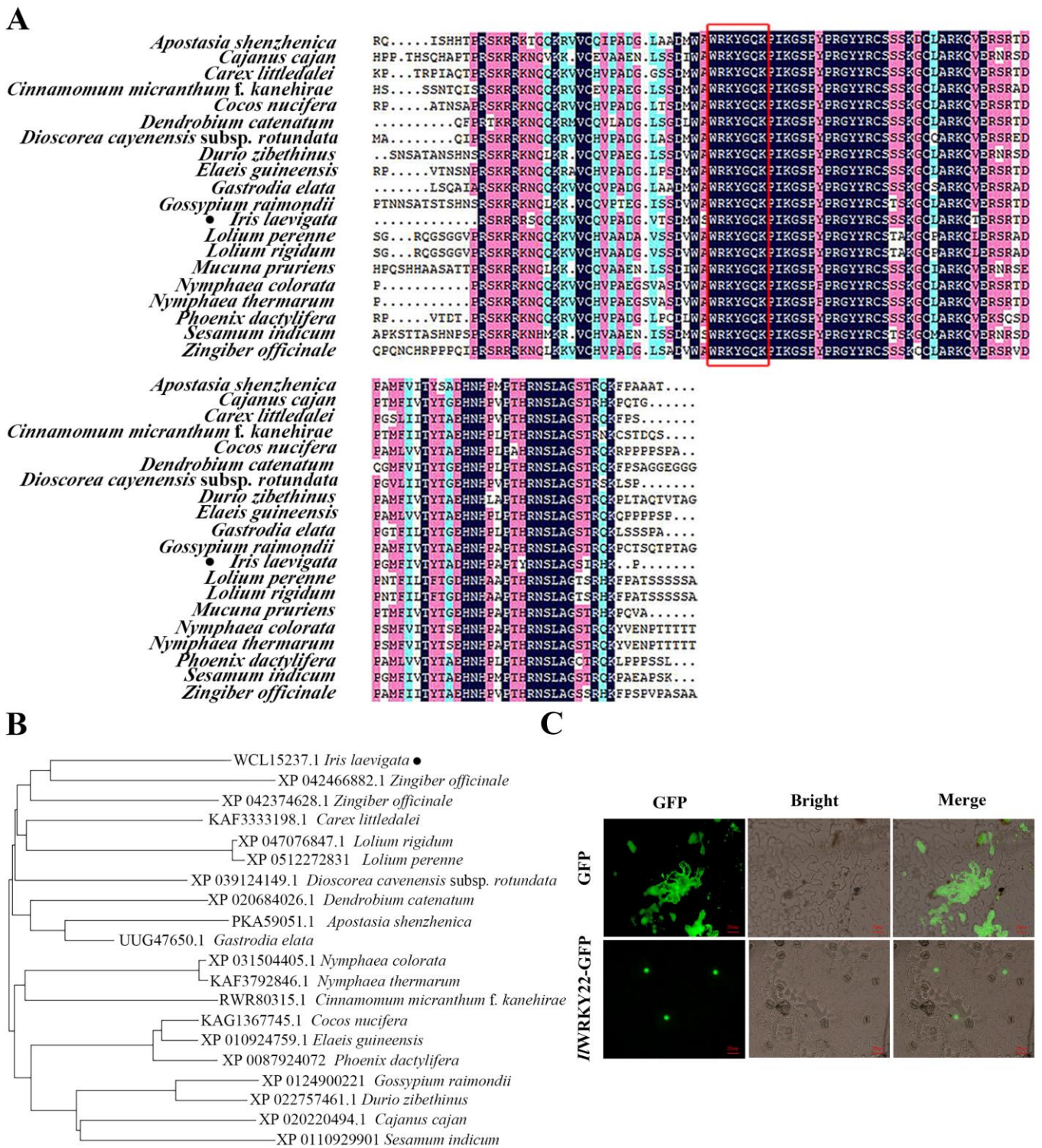


Figure 2. Sequence phylogenetic analysis and subcellular localization of IWRKY22. (A) Protein sequence alignment of IWRKY22 and that of other plant species (*Zingiber officinale*, *Zingiber officinale*, *Carex littledalei*, *Lolium rigidum*, *Lolium perenne*, *Dioscorea cayenensis* subsp. *rotundata*, *Dendrobium catenatum*, *Apostasia shenzhenica*, *Gastrodia elata*, *Nymphaea colorata*, *Nymphaea thermarum*, *Cinnamomum micranthum* f. *kanehirae*, *Cocos nucifera*, *Elaeis guineensis*, *Phoenix dactylifera*, *Gossypium raimondii*, *Durio zibethinus*, *Cajanus cajan*, and *Sesamum indicum*). The red box is the highly conserved WRKYGQK domain. Black dots indicate IWRKY22 from *I. laevigata*. Among them, purple represents 100% homologous sequence, pink represents $\geq 75\%$ homologous sequence, blue represents $\geq 50\%$ homologous sequence,

yellow represents $\geq 33\%$ homologous sequence. (B) A phylogenetic tree of *IIWRKY22*. Black dots indicate *IIWRKY22* from *I. laevigata*. (C) Subcellular localization of *IIWRKY22* protein. From left to right: GFP, bright field and merge signals. Scale bar was 20 μm .

3.3. Expression of *IIWRKY22* in *I. laevigata*

We treated one-year-old *I. laevigata* with NaCl at 300 mM and PEG-6000 at 20%. The expression of *IIWRKY22* was examined in the roots, tubers, and leaves in *I. laevigata*. A higher level of *IIWRKY22* was found in the leaves (Figure 3A). The real-time expression level of *IIWRKY22* in the leaves was detected after 0, 2, 6, 12, and 24 h; the peak expression was found 6 h after treatment with salt and 2 h after drought treatment (Figure 3B,C). Five plants were selected from each line of each treatment gradient for measurements, which were repeated three times.

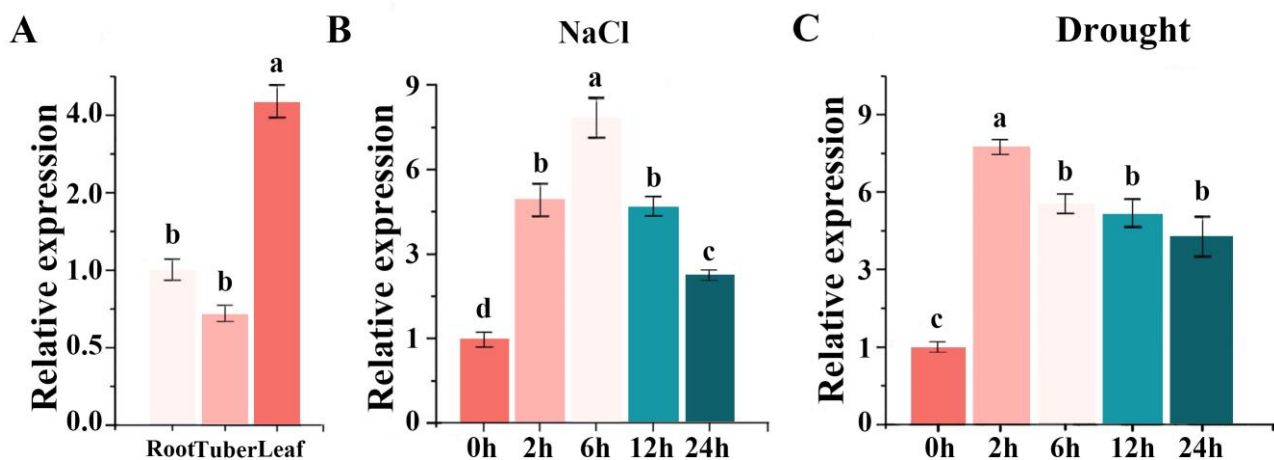


Figure 3. Expression analysis of *IIWRKY22*. (A) The expression of *IIWRKY22* was analyzed in the roots, tubers, and leaves of *I. laevigata*. (B) The expression of *IIWRKY22* was examined under NaCl stress at different time points. (C) The expression of *IIWRKY22* was evaluated in response to PEG-6000 at different time intervals. The bar chart in the figure displays the results, with different letters on top indicating significant differences between the groups ($p < 0.05$).

3.4. Overexpressing *IIWRKY22* in Both *A. thaliana* and *N. tabacum*

We obtained 14 positive transgenic *A. thaliana* lines and 10 *N. tabacum* lines, respectively, via Hyg (Xilong Scientific, Beijing, China) selection and PCR verification. These plants were allowed to self-cross for two consecutive generations, and randomly selected T3 lines of *A. thaliana* and *N. tabacum* were used for further experiments. RT-qPCR showed much-enhanced expression levels of *WRKY22* in these transgenic lines compared to the WT and empty vector (EV); three lines of both *A. thaliana* (designated as OE-1, OE-4, and OE-9) and *N. tabacum* (designated as OE-2, OE-3, and OE-5) (Figure S1) with high expression level were selected for the follow-up experiment.

3.5. Overexpressing *IIWRKY22* Delays Flowering in *A. thaliana* and *N. tabacum*

We used two plant model systems for functional validation studies. For *A. thaliana*, we focused more on the flowering phenotype. The use of *N. tabacum* for stress treatment is convenient for subsequent measurement of multiple indicators; we also used *N. tabacum* to monitor the flowering phenotype. Firstly, we compared the flowering statistics of WT, EV, and *IIWRKY22* overexpressing *A. thaliana* under short-day conditions (Figure 4A). In the WT lines, bolting time was 31.0 d, flowering time was 34.9 d, and the number of rosettes was 14.3. Similarly, the results of EV lines were 31.6 d for bolting time, 35.1 d for flowering time, and 14.8 rosettes ($p > 0.05$). In contrast, overexpression of *IIWRKY22* resulted in a significant ($p < 0.05$) delay in bolting time to 35.8 d, flowering time to 39.1 d, and an increase in the number of roseate leaves to 18.1 (Figure 4B–D). Then we compared the

flowering statistics between WT and EV *N. tabacum* as well as *IIWRKY22*-overexpressing *N. tabacum* under long-day conditions (Figure S2). The flowering times observed were found to be not significantly different with values of 62.7 d, 63.4 d for WT and EV lines, while overexpression of *IIWRKY22* further delayed flowering time to reach a value of 68.6 d (Figure S2). In summary, *IIWRKY22* was found to significantly delay flowering.

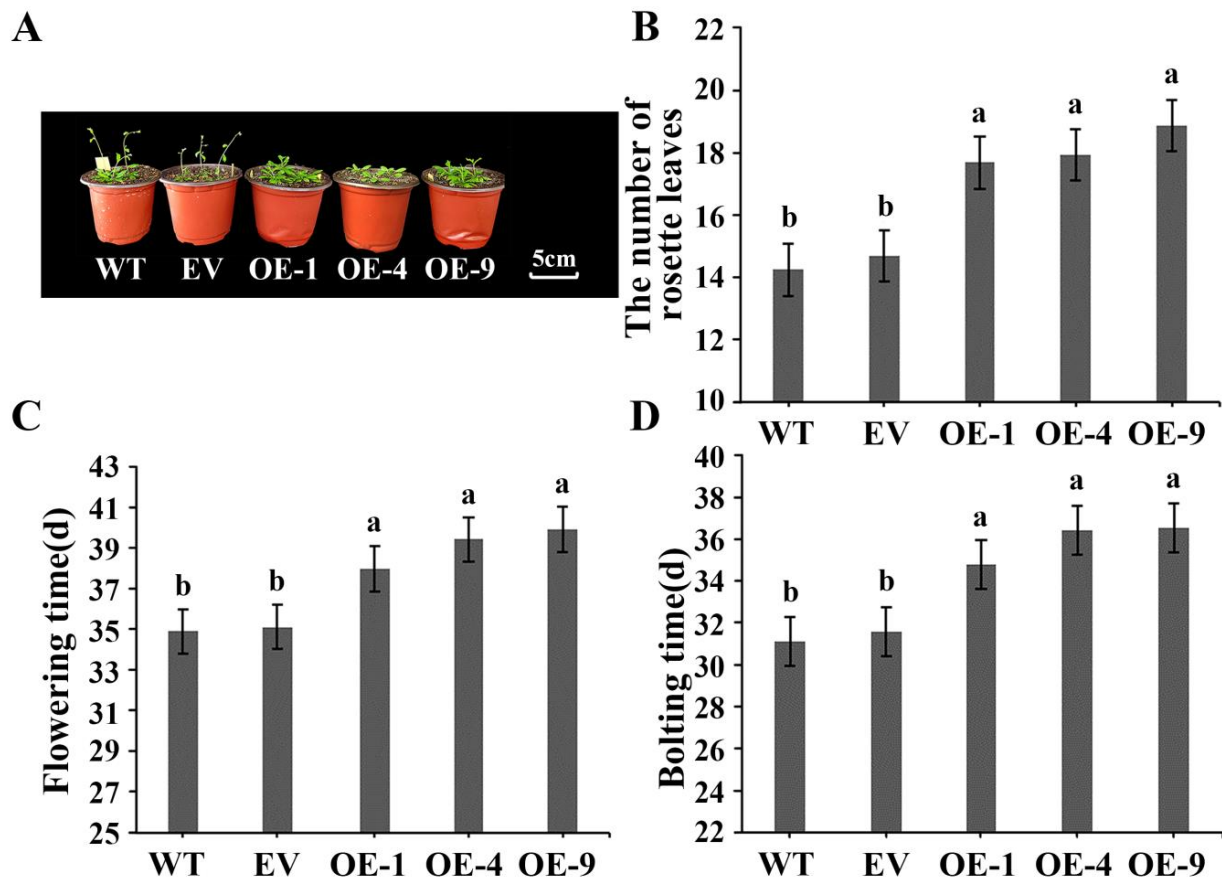


Figure 4. Phenotypes of transgenic *A. thaliana* overexpressing *IIWRKY22*. (A) Phenotypic observation of transgenic *A. thaliana* overexpressing *IIWRKY22*. Scale bar was 5 cm. (B) The number of rosette leaves at the time of flowering. (C) Flowering time (opening of the first flower). (D) Bolting time (inflorescence stalk of 1 cm). Bar graph data are Mean \pm SD, marked with different lowercase letters to indicate significant differences ($p < 0.05$). WT is wild type plants. EV is empty vector plants. OE-1, OE-4, and OE-9 are overexpressed lines of *IIWRKY22*. All these experiments were performed in triplicate.

3.6. Overexpression of *IIWRKY22* Modulates the Expression of Flowering Time Genes

To understand the molecular mechanisms by which *IIWRKY22* delays flowering, we quantified the mRNA levels of key genes in flowering pathways. On day 7, the RT-qPCR results revealed significant differences in the expression levels of key genes *CO*, *GA20OX*, *SVP*, *FLC*, and *VRN1* within the photoperiod pathway, GA pathway, and temperature pathway among WT, EV, and OE lines (Figure 5A). *CO* and *GA20OX* are significantly up-regulated, while *SVP*, *FLC*, and *VRN1* are significantly down-regulated. This suggested that *IIWRKY22* may regulate these pathways in the early flowering transition. The *FLC* protein acts as a crucial regulator of flowering, capable of integrating signals from *SVP* and *VRN1* to suppress the expression of *FT*. On day 10, *CO*, *FLC*, *SVP*, *VRN1*, and *GA20OX* are significantly up-regulated, while *FCA* are significantly down-regulated. It is speculated that with the growth of *A. thaliana*, the internal transcription environment of the expressing plant is different at different stages, so the expression level changes at day 10. The OE lines exhibited significantly elevated levels of *FLC* expression compared to the control lines (Figure 5B), which was consistent with their observed delayed flowering phenotype.

Among all the genes examined, only *GA20OX* was up-regulated in the OE plants (1.4-fold higher) compared to the WT and EV plants at day 14, while all other genes showed lower expression levels in the OE plants (Figure 5C). Notably, *SPL3* showed 80% down-regulation in the OE plants. This indicated that the OE plants were still at the early stage of flowering transition on day 14. Compared to the control group, at day 14, apart from a significant up-regulation of *GA20OX* and no significant difference in *CO* expression levels, all other genes were down-regulated in the OE strain ($p < 0.05$) (Figure 5C).

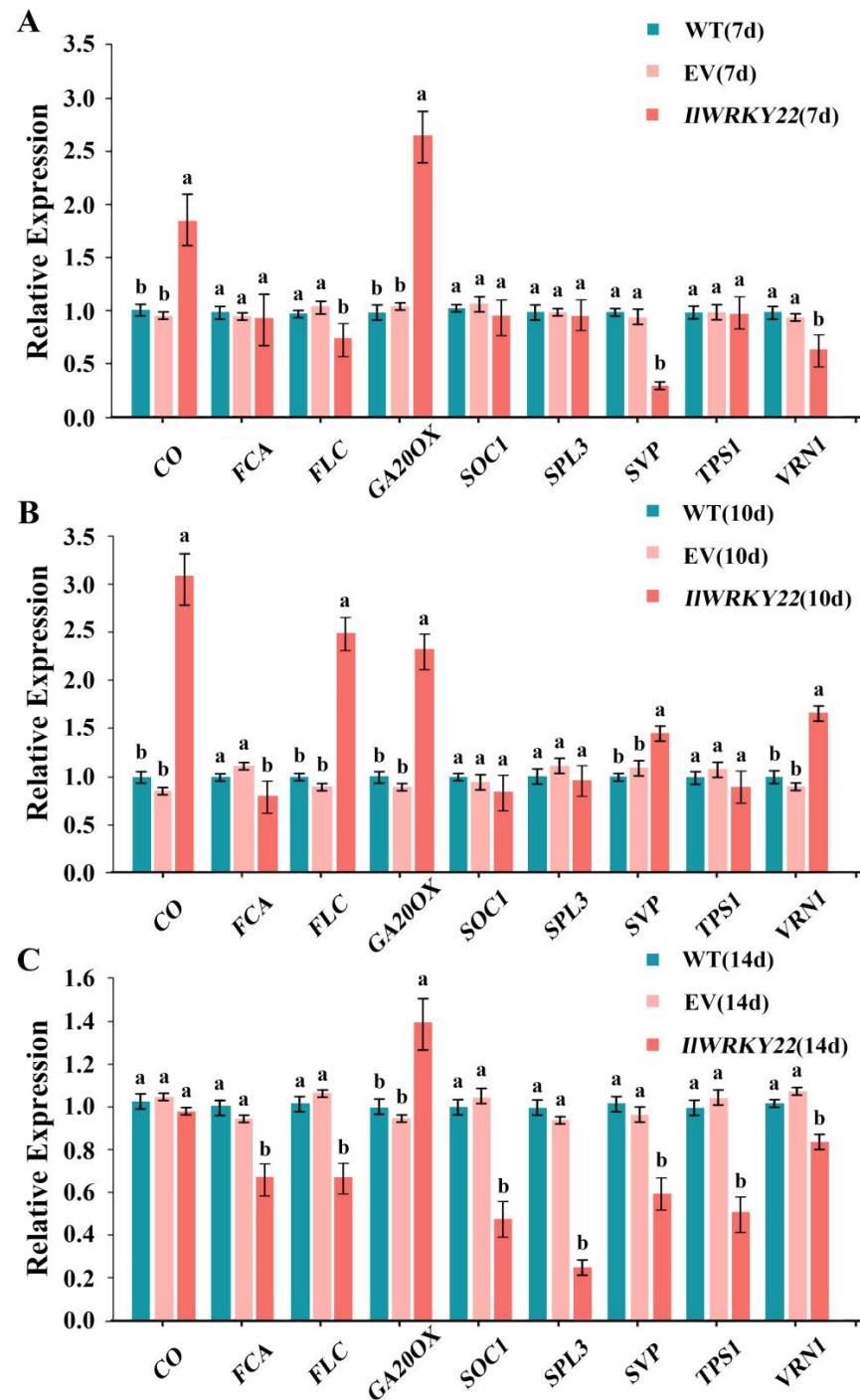


Figure 5. Expression of endogenous flowering time genes in transgenic *A. thaliana* overexpressing. (A) In 7-day-old seedlings. (B) In 10-day-old seedlings. (C) In 14-day-old seedlings. Bar graph data are Mean \pm SD, marked with different lowercase letters to indicate significant differences ($p < 0.05$). All of these experiments were performed in triplicate.

3.7. Overexpressing *IIWRKY22* in *N. tabacum* Enhances Resistance to Salt and Drought Stress

IIWRKY22 is a multifaceted gene during distinct biological processes. Thus, we next explored its role in abiotic stress [47]. WT and EV were employed as controls; OE-2, OE-3, and OE-5 (Transgenic *N. tabacum* lines with *IIWRKY22* gene) were subjected to salt and drought stress. Five plants were selected from each line of each treatment gradient for measurements, which were repeated three times. All five lines showed similar overall phenotypes under normal conditions (Figure 6A). Under salt stress, after 7 days post-treatment (dpt), the leaf growth rate of WT and EV lines was lower than that of the transgenic lines. At 14 dpt, transgenic lines were significantly taller than the control plants (Figure S3), which showed signs of yellowing and wilting of leaves; however, this led to a more severe inhibition of growth in control plants compared to the transgenic plants. Under natural drought stress, WT and EV lines showed wilting at 7 dpt. All five lines showed wilting at 14 dpt; WT and EV lines showed obvious wilting and significantly lower plant height compared to the transgenic lines.

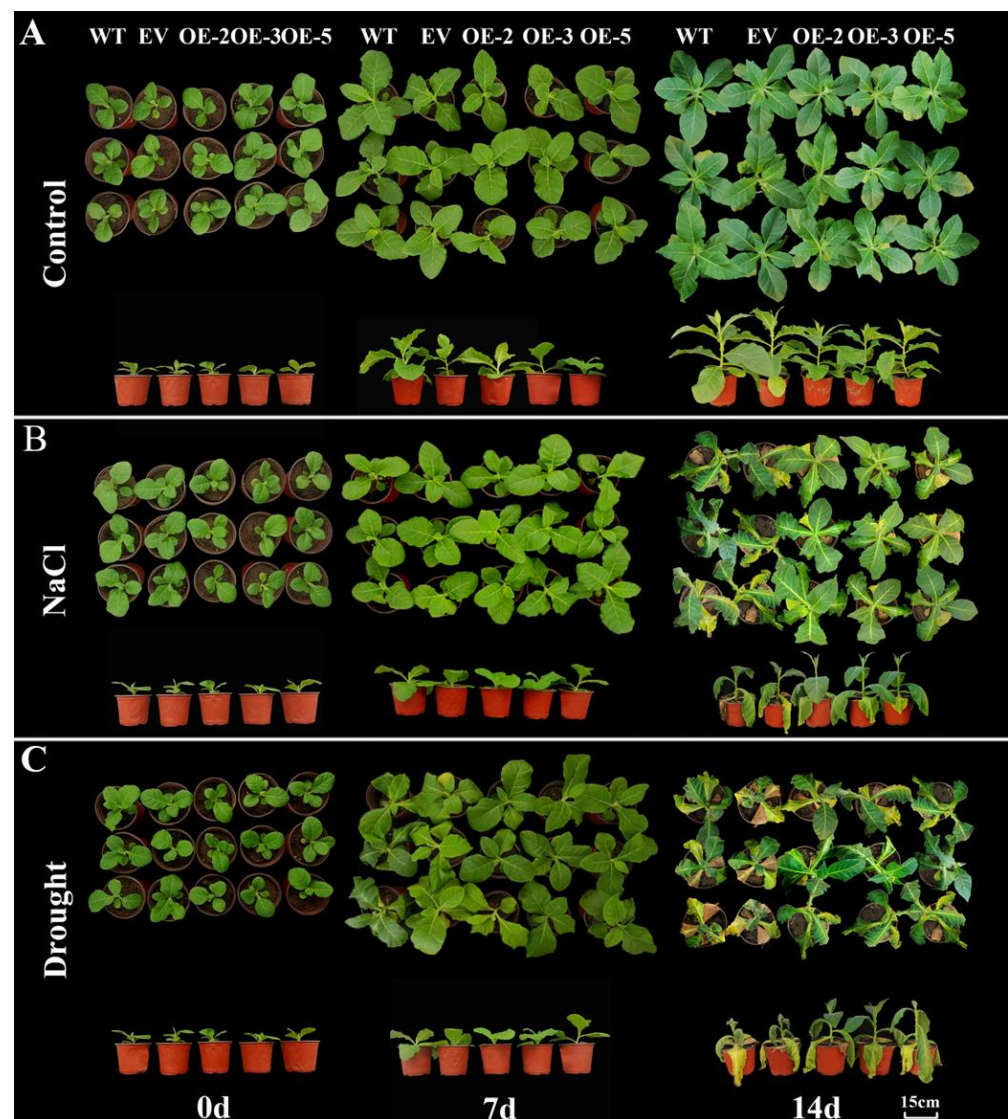


Figure 6. Overall plant phenotypes under salt and drought stress at different days post-treatment. (A) Top view and elevation of the growth state of five lines of *N. tabacum* at different in the normal growth state. (B) Top view and elevation of the growth status of five lines of *N. tabacum* at different days under NaCl stress. (C) Top view and elevation of the growth status of five lines of *N. tabacum* at different days under natural drought stress. The scale bar is 15 cm.

3.8. Impact of Overexpressing *IIWRKY22* on Photosynthesis under Salt and Drought Stress

H₂O and CO₂ are the basic raw materials for photosynthesis, which sustains normal plant growth. Gs, Chl content, Fv/Fm, Pn, Ci, and Tr are commonly used to reflect the photosynthetic capacity of plants. At the onset of salt treatment, there were no significant differences observed in various indicators ($p > 0.05$). Under salt stress, the Chl content of the five lines showed an increasing trend (Figure 7B), while Pn, Fv/Fm, Gs, Ci, and Tr gradually decreased. With the increase of the stress treatment time, the difference between the longitudinal values of the data on the 0 dpt, 7 dpt, and 14 dpt was more significant, indicating that the impact of salt stress on the photosynthesis of the plant was increasing, seriously limiting the photosynthetic capacity of the plant. However, at 7 and 14 dpt, the transgenic lines exhibited significantly higher Pn, Chl content, and Fv/Fm compared to the control lines. Conversely, Gs, Ci, and Tr were significantly lower in the transgenic lines than in the control lines during these time points (Figure 7A–F). We speculated that this might be a transgenic line that under salt stress, *IIWRKY22* alleviated the decrease in photosynthetic efficiency by increasing or maintaining the Chl content and increased the plants' water resistance under osmotic stress by closing the stomata to retain water. Similarly, there was no significant difference in the six indexes of the five lines on 0 dpt of drought stress ($p > 0.05$), and the trend was the same as that of salt stress with the increase of drought stress time, which may be because drought stress can trigger ABA synthesis in vascular tissues and guard cells. ABA signaling in guard cells regulates plasma membrane ion channels, triggering long-term outflow of negative ions and K⁺, leading to guard cell shrinkage and stomatal closure [48]. We observed a gradual decline in Pn, Fv/Fm, Gs, Ci, and Tr for all tested lines as stress progressed; these indicators reached very low levels at 14 dpt, when the five lines were already severely dehydrated compared to 0 dpt. Notably, at 7 and 14 dpt, the three overexpressing lines demonstrated significantly higher Pn values along with increased Chl content and Fv/Fm when compared to the control group ($p < 0.05$). Conversely, Gs, Ci, and Tr showed a significant decrease in these overexpressing lines relative to controls under drought conditions ($p < 0.05$) (Figure 7G–L). In summary, *IIWRKY22* can alleviate damage of transgenic *N. tabacum* induced by salt stress and drought stress, which is consistent with the observed phenotype results of transgenic tobacco under stress conditions.

3.9. *IIWRKY22* Promotes the Response of *N. tabacum* to Salt and Drought Stress

Salt and drought stress can lead to the production of reactive oxygen species (ROS) in plants, which oxidize lipids and generate MDA. Superoxide anions (O₂⁻) and H₂O₂ are the main ROS substances [49]. On the other hand, ROS and their derivatives can be counterbalanced by the antioxidant system including SOD, CAT, and POD [50]. To study the involvement of *IIWRKY22* in the ROS clearance enhanced salt and drought stress resistance, we quantified the levels of MDA, O₂⁻, and H₂O₂, as well the enzymatic activity of SOD, CAT, and POD in the leaf. The results showed that there was no significant difference in MDA, O₂⁻, and H₂O₂ contents among the five strains under 0 dpt stress. We found increasing levels of MDA, O₂⁻, and H₂O₂ in all plants as the salt/drought stress progressed (Figure 8A–C,G–I), indicating abiotic stress induced oxidative stress in plants. Under both conditions, the OE plants showed significantly lower levels of MDA, O₂⁻, and H₂O₂ at both 7 and 14 dpt compared to the control plants ($p < 0.05$). NBT and DAB can directly show the amount of O₂⁻ and H₂O₂ accumulation through the change of color. At 0 dpt, MDA, O₂⁻, and H₂O₂ contents of the five lines were not significantly different ($p > 0.05$), and the color of the plants was gradually deepened with the stress time, which indicated that O₂⁻ and H₂O₂ accumulated more with the passing of time and the plants were subjected to more stress. NBT and DAB staining also showed less O₂⁻ and H₂O₂ accumulation in the OE plants compared to the WT and EV plants (Figure 8M,N). There was no significant difference in SOD, CAT, and POD at 0 dpt ($p > 0.05$). The difference was that with the increase of time, the activity levels of three enzymes in OE plants were higher than those in the control group (WT, EV), and the ROS levels were lower (Figure 8D–F,J–L). These results

indicated that the *N. tabacum* overexpressing *IIWRKY22* had a stronger ability to remove ROS and accumulate fewer harmful substances under salt and drought stresses than the control and could better cope with salt and drought stresses.

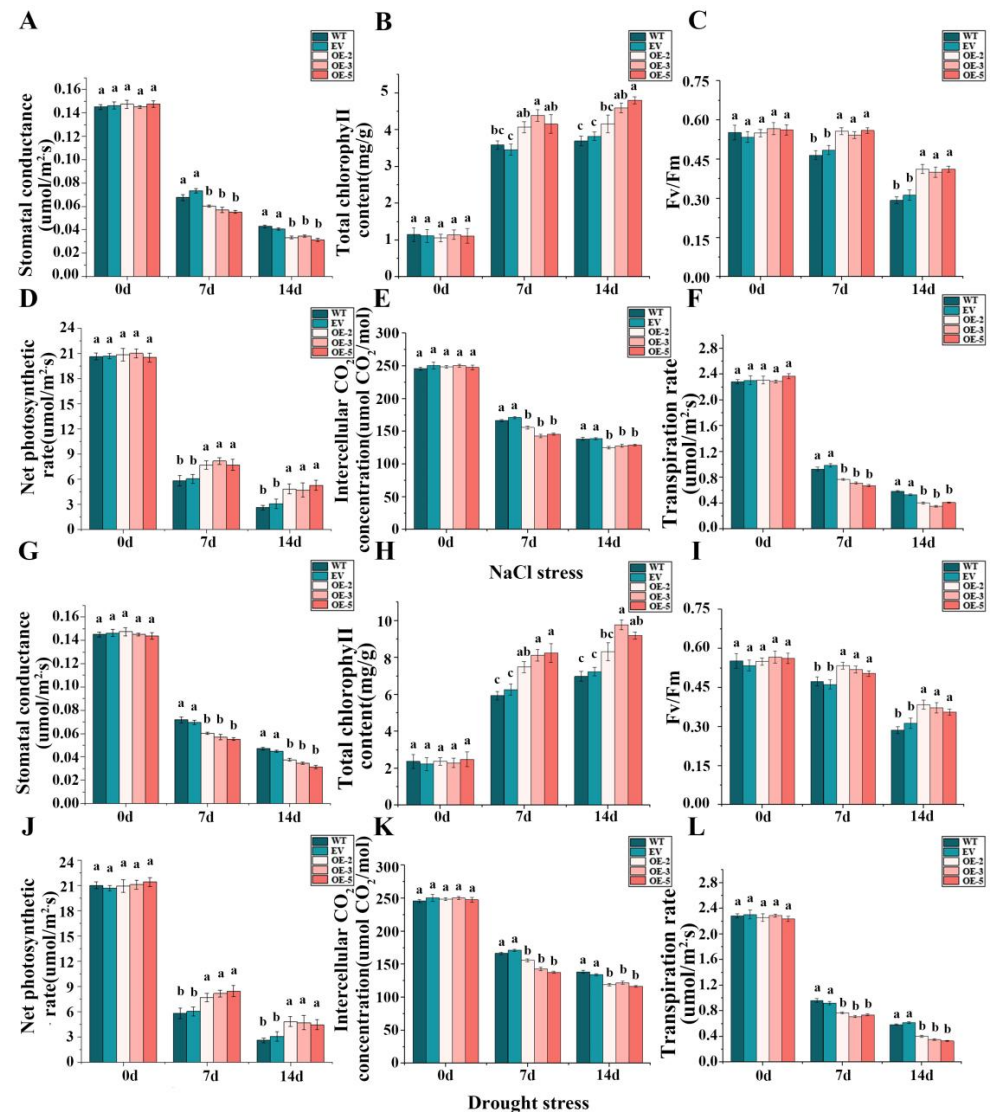


Figure 7. Impact of overexpressing *IIWRKY22* on photosynthetic and transpiration rate indexes under salt and drought stress. (A–F) G_s , Chl content, Fv/Fm, Pn, Ci, and Tr of *N. tabacum* five lines at different days under NaCl stress. (G–L) G_s , Chl content, Fv/Fm, Pn, Ci, and Tr of *N. tabacum* five lines at different days under natural drought. Different letters above the bars indicated significant differences ($p < 0.05$). WT is wild type plants. EV is empty vector plants. OE-2, OE-3, and OE-5 are overexpressed lines of *IIWRKY22*. All these experiments were performed in triplicate.

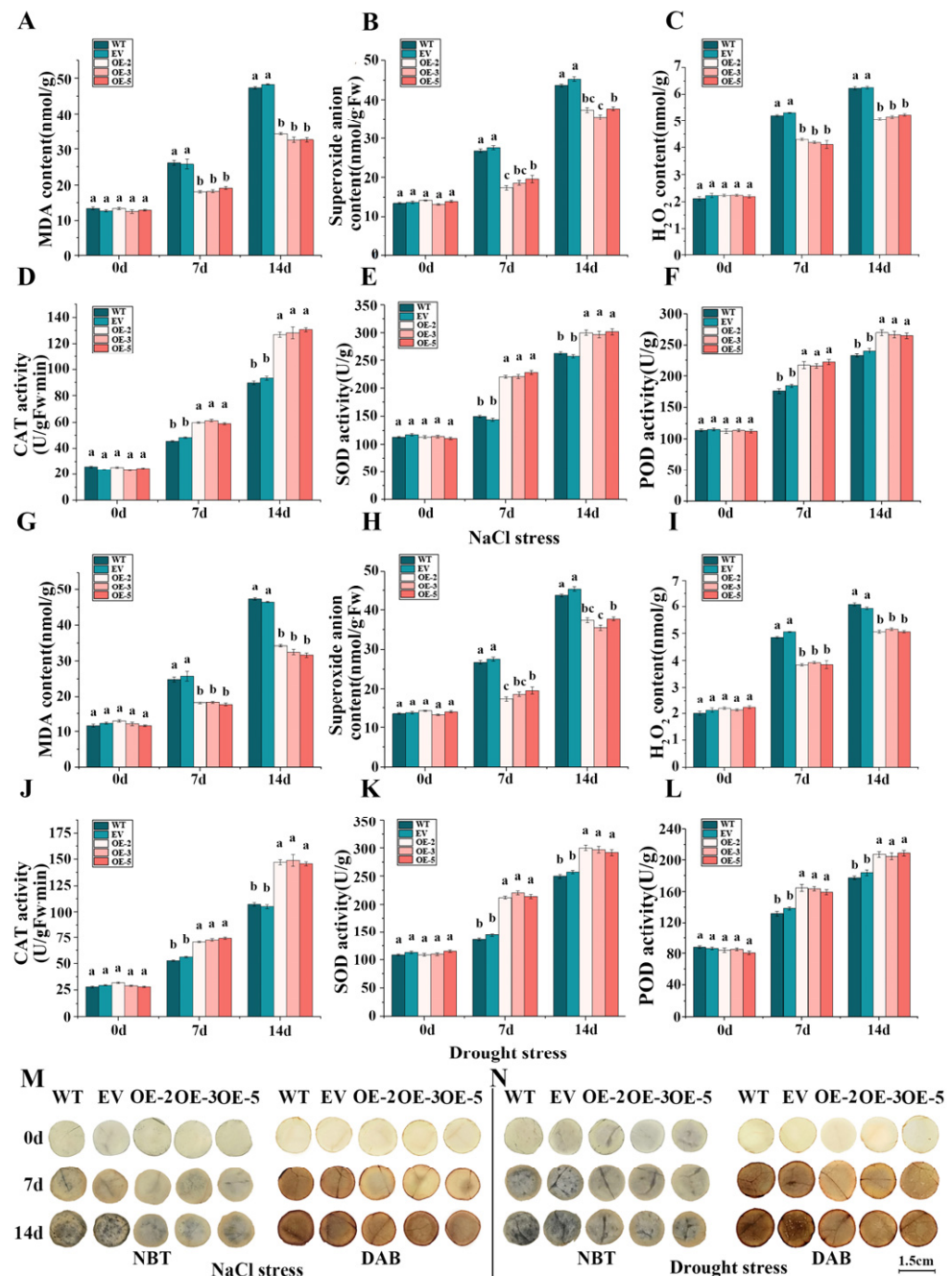


Figure 8. Involvement of ROS regulation. Analysis of physiological indexes of *N. tabacum* seedlings overexpressing *IIWRKY22* under salt stress and drought stress. (A–F) The contents of MDA, O₂⁻, H₂O₂ and the activities of CAT, SOD, and POD in *N. tabacum* five lines leaves were measured at different days after NaCl stress. (G–L) The contents of MDA, O₂⁻, H₂O₂ and the activities of CAT, SOD, and POD in *N. tabacum* five lines leaves were measured at different days of natural drought stress. Different letters on the bar chart represent significant differences ($p < 0.05$). (M) Plot of leaf disc staining using NBT and DAB in five lines at different days of NaCl stress. (N) Leaf disc staining plots using NBT and DAB in five lines at different days of natural drought stress. A deeper NBT staining indicates a higher accumulation of O₂⁻, while a deeper DAB staining indicates a greater accumulation of H₂O₂. Consequently, increased levels of both O₂⁻ and H₂O₂ accumulation led to more severe plant damage. The scale bar is 1.5 cm.

3.10. The *IIWRKY22* on Expression Levels of Stress-Related Genes *NtCAT*, *NtHAK1*, *NtPMA4*, *NtPOD*, *NtSOD*, and *NtSOS1* under Salt and Drought Stress

To further investigate the role of *IIWRKY22* in enhancing tolerance to salt and drought stress, we quantified the relative expression levels of stress-related genes. Our results revealed that *NtCAT*, *NtHAK1*, *NtPMA4*, *NtPOD*, *NtSOD*, and *NtSOS1* were significantly up-regulated under both salt and drought stress, regardless of the genetic background (Figure 9). We found that the relative expression levels of these genes were significantly up-regulated in all the tobacco plants at 7 and 14 dpt, but the increase of each gene in the OE-2, OE-3 and OE-5 lines was significantly higher than that of the WT and EV at both time points. However, OE lines showed the highest degree of increase at both 7 and 14 dpt compared to that of the control plants.

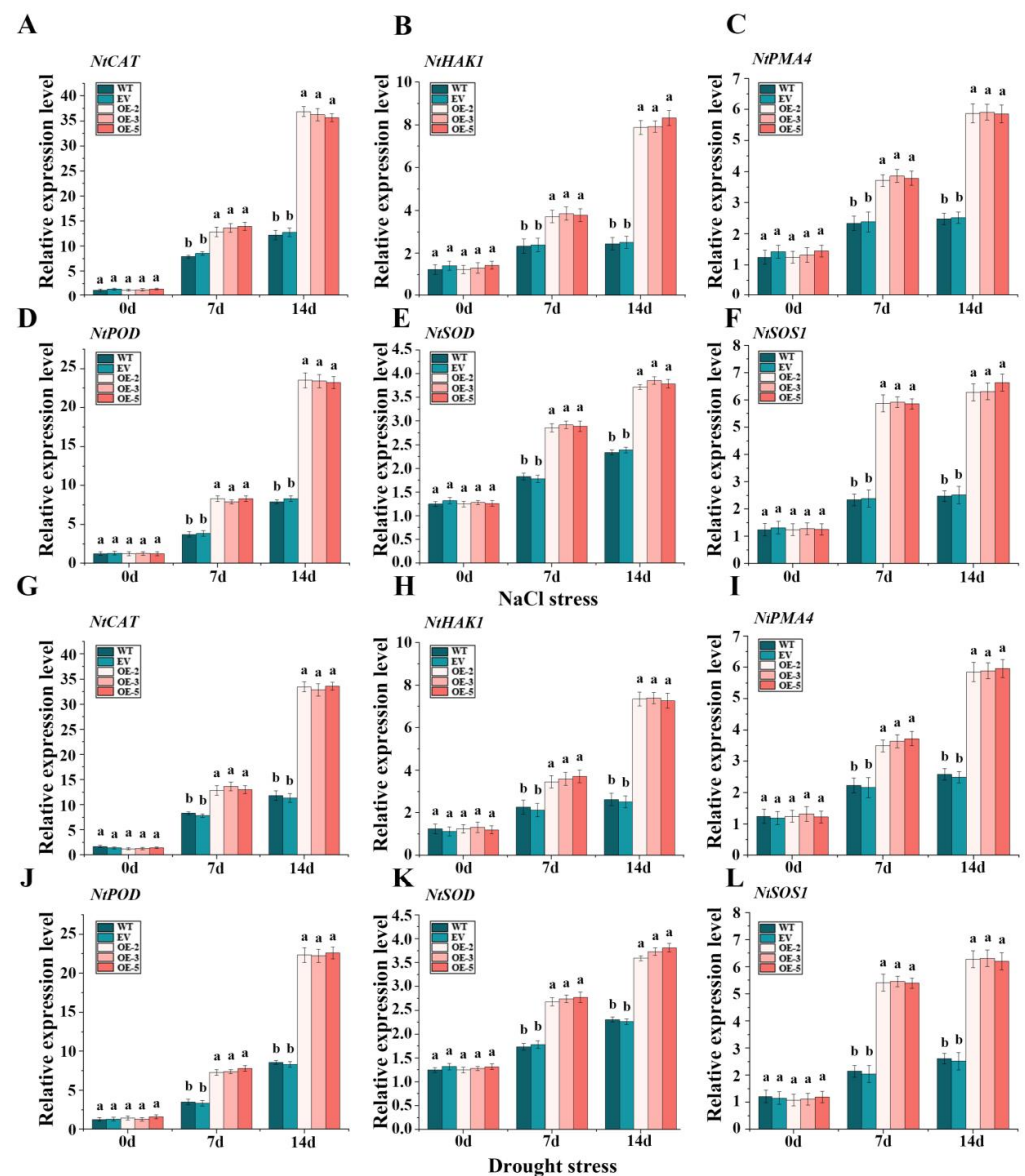


Figure 9. Expression of salt and drought stress-responsive genes in overexpressed *IIWRKY22* *N. tabacum*. (A–F) The expression levels of *NtCAT*, *NtHAK1*, *NtPMA4*, *NtPOD*, *NtSOD*, and *NtSOS1* gene in five lines at different days under 300 mM NaCl. (G–L) The expression levels of *NtCAT*, *NtHAK1*, *NtPMA4*, *NtPOD*, *NtSOD*, and *NtSOS1* gene in five lines at different days under natural drought. Different letters above the bars indicated significant differences ($p < 0.05$).

4. Discussion

Using our *I. laevigata* transcriptome data from the tepals, we identified a total of 68 WRKYs and classified them into three groups: 22 in Group I, 35 in Group II, and 11 in Group III. These three groups of WRKYs may participate in various biological processes or pathways based on previous functional studies in multiple plant species (Table S2). The functional redundancy of these WRKYs indicates their key roles in responding to both external and internal stimuli [51]. It can also be reflected by the presence of redundant sequences in many plant species including *Xanthoceras sorbifolium* Bunge. [52] and *Solanum lycopersicum* L. [53], possibly due to duplication during plant evolution. Indeed, several sub-genome duplication events may have led to the formation of a large WRKY family in most modern eukaryotes [33].

IIWRKY22 may be a multifaceted TF controlling multiple traits [13,18,19,54]. Thus, we selected it for functional studies. We focused on its role in flowering and found that overexpressing *IIWRKY22* delays flowering in *A. thaliana* and *N. tabacum*. This provides another line of evidence to support the key roles of WRKYs in controlling flowering time. For example, heterologous expression of the cotton *GbWRKY1* gene in *A. thaliana* promotes flowering by regulating the transcription of *SOC1* [12]. Similarly, an up-regulation of *BcWRKY22* in Chinese cabbage by low temperature promotes bolting and flowering via increasing *BcSOC1* [55] and metabolism of other players for flowering control including *SPL3*. A lower-level expression of *SPL3* in the transgenic plants may further lead to a down-regulation of *SOC1*, which ultimately causes a delay in the environment and initiates dynamic regulation of flowering [56].

Corresponding to the multiple environmental aspects affecting flowering, plants evolved multiple flowering transition pathways including the de-repression of *CDF* on *CO* and *FT* by the photoperiod pathway; the de-repression of *FLC* on *FT* in the vernalization, temperature, and autonomous pathways; as well as the de-repression of *SOC1* by degrading DELLA proteins in the GA pathway. To delineate the exact mechanisms in which *IIWRKY22* was involved, we quantified the expression of 10 genes in multiple pathways (Figure 5). Our data showed a significant up-regulation of *CO* and *GA20OX*, indicating that the primary networks downstream of *IIWRKY22* were the photoperiod pathway and the GA pathway [48]. This in turn resulted in altered metabolism of other players for flowering control including *SPL3*. A lower-level expression of *SPL3* in the transgenic plants may further lead to a down-regulation of *SOC1*, which ultimately causes a delay in flowering. Interestingly, *SPL3* is a major effector in the aging pathway as overexpressing or knocking-out dark-treated *AtWRKY22* led to accelerated and delayed senescence phenotypes, respectively, in *A. thaliana* [54]. Thus, it raises the possibility that *IIWRKY22* regulates flowering transition via the aging pathway and that *IIWRKY22* is the converging point of multiple pathways including flowering and senescence.

In addition to flowering control, *WRKY22* also plays a role in abiotic stress in plants. For example, *CsWRKY22* in *Citrus sinensis* regulates susceptibility to canker disease [57], *LiWRKY22* can promote heat resistance of *lily* [58]; *CmWRKY22* has a positive regulatory effect in response to drought stress [59]. Our study further revealed a role of *IIWRKY22* in responding to salt and drought stress [60]. Compared to controls, plants overexpressing *IIWRKY22* showed much-improved growth under both salt and drought stress (Figure 6). This is in line with the finding that *WRKY22* is significantly up-regulated by drought stress. The enhanced resistance to salt and drought stress can be attributed to up-regulation in photosynthesis (higher Chl content, Pn, and Fv/Fm compared to the control plants) and water retention capacity (lower Gs, Ci, and Tr, Figure 7). In this case, overexpressing *IIWRKY22* in *N. tabacum* still has higher photosynthetic capacity and water retention capacity compared with WT *N. tabacum*, as indicated by relatively higher Chl content and lower Gs. This is consistent with a previous report [61]. The lower Ci in transgenic plants can be explained by higher photosynthetic activities [39]. The ability of *IIWRKY22* in enhancing the resistance of *N. tabacum* to salt or drought stress and maintaining growth in stress environments are interconnected. Photosynthesis is an important indicator of the

ability of plants to respond to abiotic stress [62]. Under high-salt and drought conditions, plants in general lose water due to high osmotic pressure, leading to stomatal closing, disrupted chloroplast structures, decreased activity of chlorophyll enzymes, and eventually inhibition of photosynthesis [63–65]. Manipulating the expression of protective genes and thus the regulation of gene networks may confer a better resistance. Our data suggested that the protective role of *IIWRKY22* involved multiple processes that can alleviate the adverse impact of salt and drought stress.

Although the exact molecular mechanisms by which *IIWRKY22* protects plants against salt and drought stress are not clear, one possible mechanism is via ROS regulation. This is evidenced by the observation that the transgenic plants overexpressing *IIWRKY22* accumulate less O_2^- , H_2O_2 , and MDA compared to that of the control plants (Figure 8). The generation of ROS and secondary damage to the cell membrane including membrane lipid peroxidation under environmental challenges have been well documented in plants [66,67]. By lowering the level of oxidative stress, *IIWRKY22* may protect plants from excessive damage to the cellular membrane under stress. In addition, numerous studies have shown the key role of antioxidant enzymes including SOD, POD, and CAT in counterbalancing ROS in plants [66,68]. Consistent with these studies, we found that the enzyme activities of SOD, CAT, and POD were increased in *IIWRKY22*-overexpressing plants under stress (Figure 8). In summary, both an increase in antioxidant enzyme activity and a decrease in ROS accumulation led to a lower level of oxidative stress under salt and drought treatment in transgenic plants, which contributed to a better photosynthetic capacity and enhanced resistance under unfavorable conditions.

To further investigate the role of *IIWRKY22* under salt and natural drought stress, we examined the expression levels of several key genes associated with plant stress tolerance in transgenic plants overexpressing *IIWRKY22* following stress induction. Our results revealed a significant up-regulation of *NtCAT*, *NtHAK1*, *NtPMA4*, *NtPOD*, *NtSOD*, and *NtSOS1* in the transgenic *N. tabacum* plants compared to the control plants. This suggests that *IIWRKY22* may directly or indirectly regulate the expression of downstream stress response genes. Salt overly sensitive 1 (SOS1) plays a crucial role in facilitating the efflux of Na^+ ions from cells, thereby protecting plants from salt-induced toxicity caused by excessive intracellular Na^+ accumulation [69]. Plasma membrane H^+ -ATPase4 (PMA4) is involved in regulating cellular K^+ uptake and maintaining appropriate K^+ concentration [70]. Additionally, the high affinity potassium transporter1 (HAK1) helps balance intracellular Na^+/K^+ levels and prevents excessive intracellular Na^+ content from causing cellular toxicity [71].

5. Conclusions

IIWRKY22 has the dual function of flowering time control and regulation in salt and drought stress. Overexpressing *IIWRKY22* in *A. thaliana* and *N. tabacum* causes a delay in flowering via the effect of the expression of *CO*, *GA20OX*, *SPL3*, and *SOC1*. In addition, overexpression of *IIWRKY22* in *N. tabacum* enhances the tolerance to salt and drought treatment by positively regulating the antioxidant system and photosynthesis. Thus, *IIWRKY22* is a promising candidate for breeding *Iris*, as it has the potential to delay the flowering period of *Iris* and enhance the plant's resistance to salt and drought.

Supplementary Materials: The following supporting information can be downloaded at: <https://www.mdpi.com/article/10.3390/plants13091191/s1>. Supplemental Figure S1. Gene expression profile of *IIWRKY22* transgenic T3 generation plants. (A) Relative expression of *IIWRKY22* in fourteen T3 transgenic *A. thaliana* lines. (B) Relative expression of *IIWRKY22* in ten T3 transgenic *N. tabacum* lines. Supplemental Figure S2. Phenotypes of transgenic *N. tabacum* overexpressing *IIWRKY22*. (A) Phenotypic observation of transgenic *N. tabacum* overexpressing *IIWRKY22*. Scale bar was 15 cm. (B) Flowering time (opening of the first flower). Bar graph data are Mean \pm SD, marked with different lowercase letters to indicate significant differences ($p < 0.05$). Supplemental Figure S3. Overall plant height under salt and drought stress at 0, 7, and 14 dpt. (A) Plant height observation of WT, EV, and OE lines of *N. tabacum* at 0, 7, and 14 days in the normal growth state. (B) Plant height observation of WT, EV, and OE lines of *N. tabacum* at 0, 7, and 14 days under NaCl stress at 300 mM. (C) Plant

height observation of WT, EV, and OE lines of *N. tabacum* at 0, 7, and 14 days under natural drought stress. Bar graph data are Mean \pm SD, marked with different lowercase letters to indicate significant differences ($p < 0.05$). Supplemental Table S1. Primer sequence and application. Supplemental Table S2. Functional prediction of WRKY transcription factor family members in *I. laevigata*. Supplemental Table S3. Abbreviations.

Author Contributions: Conceptualization, L.F. and S.Z.; methodology, L.F., Z.N. and G.S.; software, L.F., Z.N., G.S., Z.S. and Q.Y.; validation, L.F., Z.N., G.S., Z.S. and Q.Y.; formal analysis, L.W.; investigation, L.F., Z.N. and G.S.; resources, Z.S. and Q.Y.; data curation, Z.S., Q.Y. and S.Z.; writing—original draft, L.F., Z.N. and G.S.; writing—review & editing, L.W.; visualization, Z.S., Q.Y. and S.Z.; supervision, L.W.; funding acquisition, L.W. All authors have read and agreed to the published version of the manuscript.

Funding: This study was supported by the Fundamental Research Funds for the Central Universities (2572023CT18) and the Natural Fund Project of Heilongjiang Province (LH2021C017).

Data Availability Statement: Data from this study are available from the corresponding author upon reasonable request.

Conflicts of Interest: The authors declare no conflicts of interest.

References

- Wellmer, F.; Riechmann, J.L. Gene networks controlling the initiation of flower development. *Trends Genet.* **2010**, *26*, 519–527. [[CrossRef](#)] [[PubMed](#)]
- Rehman, S.; Bahadur, S.; Xia, W. An overview of floral regulatory genes in annual and perennial plants. *Gene* **2023**, *885*, 147699. [[CrossRef](#)] [[PubMed](#)]
- He, Y.; Chen, T.; Zeng, X. Genetic and epigenetic understanding of the seasonal timing of flowering. *Plant Commun.* **2020**, *1*, 100008. [[CrossRef](#)] [[PubMed](#)]
- Kozlov, K.; Singh, A.; Berger, J.; Bishop-von, W.E.; Kahraman, A.; Aydogan, A.; Cook, D.; Nuzhdin, S.; Samsonova, M. Non-linear regression models for time to flowering in wild chickpea combine genetic and climatic factors. *BMC Plant Biol.* **2019**, *19*, 94. [[CrossRef](#)]
- Wang, F.; Li, S.; Kong, F.; Lin, X.; Lu, S. Altered regulation of flowering expands growth ranges and maximizes yields in major crops. *Front. Plant Sci.* **2023**, *14*, 1094411. [[CrossRef](#)]
- Shah, S.; Weinholdt, C.; Jedrusik, N.; Molina, C.; Zou, J.; Grosse, I.; Schiessl, S.; Jung, C.; Emrani, N. Whole-transcriptome analysis reveals genetic factors underlying flowering time regulation in rapeseed (*Brassica napus* L.). *Plant Cell Environ.* **2018**, *41*, 1935–1947. [[CrossRef](#)]
- Liu, Y.P.; Yang, J.; Yang, M.F. Pathways of flowering regulation in plants. *Chin. J. Biol.* **2015**, *31*, 1553–15666.
- Liang, H.M.; Xia, Y.; Wang, T.M. Research Progress on Genetic Engineering of Plant Cold Resistance, Drought Resistance and Salt Tolerance. *Acta Pratac. Sin.* **2003**, *3*, 1–7.
- Sun, Y.; Zhou, J.; Guo, J. Advances in the knowledge of adaptive mechanisms mediating abiotic stress responses in *Camellia sinensis*. *Front. Biosci.* **2021**, *26*, 1714–1722. [[CrossRef](#)]
- Zhu, J.K. Abiotic stress signaling and responses in plants. *Cell* **2016**, *167*, 313–324. [[CrossRef](#)]
- Biswas, T.; Islam, M.A.; Haque, T. Exogenously applied moringa leaf extracts and mixed fertilizers in soil to improve growth and yield of tomato (*Lycopersicon esculentum* Mill.). *Sustain. Food Agric.* **2020**, *1*, 42–47. [[CrossRef](#)]
- Luo, X.; Li, C.; He, X.; Zhang, X.; Zhu, L. ABA signaling is negatively regulated by *GbWRKY1* through JAZ1 and ABI1 to affect salt and drought tolerance. *Plant Cell Rep.* **2020**, *39*, 181–194. [[CrossRef](#)] [[PubMed](#)]
- Su, W.; Xiao, L.Y.; Sun, G.W.; Liu, H.C.; Song, S.W.; Chen, R.Y. Functional analysis of transcription factor *BCWRKY22* in low temperature-induced bolting and flowering of *Brassica campestris*. *Mol. Breed.* **2020**, *18*, 3862–3870.
- Li, J.; Han, G.; Sun, C.; Sui, N. Research advances of MYB transcription factors in plant stress resistance and breeding. *Plant Signal. Behav.* **2019**, *14*, 1613131. [[CrossRef](#)] [[PubMed](#)]
- Golldack, D.; Luking, I.; Yang, O. Plant tolerance to drought and salinity: Stress regulating transcription factors and their functional significance in the cellular transcriptional network. *Plant Cell Rep.* **2011**, *30*, 1383–1391. [[CrossRef](#)] [[PubMed](#)]
- Fedoroff, N.V.; Battisti, D.S.; Beachy, R.N.; Cooper, P.J.; Fischhoff, D.A.; Hodges, C.N.; Knauf, V.C.; Lobell, D.; Mazur, B.J.; Molden, D.; et al. Radically rethinking agriculture for the 21st century. *Science* **2010**, *327*, 833–834. [[CrossRef](#)] [[PubMed](#)]
- Xia, Y.; Huang, G.; Zhu, Y. Sustainable plant disease control: Biotic information flow and behavior manipulation. *Sci. China-Life Sci.* **2019**, *62*, 1710–1713. [[CrossRef](#)]
- Ma, J.J. Cloning and Preliminary Function Analysis of *Hawrky9/14/22/30/79* Genes in *Helianthus annuus*. Master's Thesis, Harbin Normal University, Harbin, China, 2022; p. 001596.
- Chen, Y.P.; Lin, J.H.; Liu, Z.Q.; He, S.L.; She, W.Q.; Chen, G.X. Cloning and functional identification of promoter of *PsWRKY22* gene in *Prunus salicina*. *Mol. Breed.* **2021**, *19*, 2837–2845.

20. Khoso, M.A.; Hussain, A.; Ritonga, F.N.; Ali, Q.; Channa, M.M.; Alshegaihi, R.M.; Meng, Q.; Ali, M.; Zaman, W.; Brohi, R.D.; et al. WRKY transcription factors (TFs): Molecular switches to regulate drought, temperature, and salinity stresses in plants. *Front. Plant Sci.* **2022**, *13*, 1039329. [[CrossRef](#)]
21. Phukan, U.J.; Jeena, G.S.; Shukla, R.K. WRKY transcription factors: Molecular regulation and stress responses in plants. *Front. Plant Sci.* **2016**, *7*, 760. [[CrossRef](#)]
22. Agarwal, P.; Reddy, M.P.; Chikara, J. WRKY: Its structure, evolutionary relationship, DNA-binding selectivity, role in stress tolerance and development of plants. *Mol. Biol. Rep.* **2011**, *38*, 3883–3896. [[CrossRef](#)] [[PubMed](#)]
23. Jiang, J.; Ma, S.; Ye, N.; Jiang, M.; Cao, J.; Zhang, J. WRKY transcription factors in plant responses to stresses. *J. Integr. Plant Biol.* **2017**, *59*, 86–101. [[CrossRef](#)] [[PubMed](#)]
24. Chen, X.; Li, C.; Wang, H.; Guo, Z. WRKY transcription factors: Evolution, binding, and action. *Phytopathol. Res.* **2019**, *1*, 13. [[CrossRef](#)]
25. Bakshi, M.; Oelmüller, R. WRKY transcription factors: Jack of many trades in plants. *Plant Signal. Behav.* **2014**, *9*, e27700. [[CrossRef](#)] [[PubMed](#)]
26. Liu, G.; Li, F.; Shi, G.; Wang, L.; Wang, L.; Fan, L. Identification of MADS-Box transcription factors in *Iris laevis* and functional assessment of *ILSEP3* and *ILSVP* during flowering. *Int. J. Mol. Sci.* **2022**, *23*, 9950. [[CrossRef](#)] [[PubMed](#)]
27. Yang, J.; Yu, S.; Shi, G.F.; Yan, L.; Lv, R.T.; Ma, Z.; Wang, L. Comparative analysis of R2R3-MYB transcription factors in the flower of *Iris laevis* identifies a novel gene regulating tobacco cold tolerance. *Plant Biol.* **2022**, *24*, 1066–1075. [[CrossRef](#)] [[PubMed](#)]
28. Chen, K.; Wang, Y.; Zhang, R.; Zhang, H.; Gao, C. CRISPR/Cas Genome editing and precision plant breeding in agriculture. *Annu. Rev. Plant Biol.* **2019**, *70*, 667–697. [[CrossRef](#)]
29. Kourelis, J.; van der Hoorn, R.; Sueldo, D.J. Decoy engineering: The next step in resistance breeding. *Trends Plant Sci.* **2016**, *21*, 371–373. [[CrossRef](#)] [[PubMed](#)]
30. Tribhuvan, K.U.; Mishra, T.; Kaur, S. Identification and characterization of novel drought-responsive lncRNAs in stone apple (*Aegle marmelos* L.) through whole-transcriptome analysis. *Curr. Plant Biol.* **2024**, *38*, 100336. [[CrossRef](#)]
31. Zeng, J.; Wang, Y.; Wu, G. Comparative Transcriptome Analysis Reveals the Genes and Pathways Related to Wheat Root Hair Length. *Int. J. Mol. Sci.* **2024**, *25*, 2069. [[CrossRef](#)]
32. Wang, Y.; Xun, H.; Wang, L. Identification of Key Genes Associated with 1,2,6-Tri-O-galloyl-beta-D-glucopyranose Accumulation in *Camellia sinensis* Based on Transcriptome Sequencing. *Foods* **2024**, *13*, 495. [[CrossRef](#)] [[PubMed](#)]
33. Zhang, Y.; Wang, L. The WRKY transcription factor superfamily: Its origin in eukaryotes and expansion in plants. *BMC Evol. Biol.* **2005**, *5*, 1. [[CrossRef](#)] [[PubMed](#)]
34. Ramos, R.N.; Zhang, N.; Lauff, D.B. Loss-of-function mutations in *WRKY22* and *WRKY25* impair stomatal-mediated immunity and PTI and ETI responses against *Pseudomonas syringae* pv. tomato. *Plant Mol. Biol.* **2023**, *112*, 161–177. [[CrossRef](#)] [[PubMed](#)]
35. Zhou, L.X.; Cao, H.X. Expression characteristics of WRKY transcription factor gene in oil palm under low temperature stress. *J. South. Agric.* **2018**, *49*, 1490–1497.
36. Srikanth, A.; Schmid, M. Regulation of flowering time: All roads lead to Rome. *Cell. Mol. Life Sci.* **2011**, *68*, 2013–2037. [[CrossRef](#)] [[PubMed](#)]
37. Collings, D.A. Subcellular localization of transiently expressed fluorescent fusion proteins. *Methods Mol. Biol.* **2013**, *1069*, 227–258. [[PubMed](#)]
38. Wang, H.; Liu, Z.; Xie, J.; Li, J.; Zhang, J.; Yu, J.; Hu, L.; Zhang, G. The *CaALAD* gene from pepper (*Capsicum annuum* L.) confers chilling stress tolerance in transgenic *Arabidopsis* plants. *Front. Plant Sci.* **2022**, *13*, 884990. [[CrossRef](#)] [[PubMed](#)]
39. Wang, Y.; Cao, S.; Guan, C.; Kong, X.; Wang, Y.; Cui, Y.; Liu, B.; Zhou, Y.; Zhang, Y. Overexpressing the NAC transcription factor *LpNAC13* from *Lilium pumilum* in tobacco negatively regulates the drought response and positively regulates the salt response. *Plant Physiol. Biochem.* **2020**, *149*, 96–110. [[CrossRef](#)] [[PubMed](#)]
40. Chen, Y.; Zhang, L.; Zhang, H.; Chen, L.; Yu, D. *ERF1* delays flowering through direct inhibition of Flowering locus T expression in *Arabidopsis*. *J. Integr. Plant Biol.* **2021**, *63*, 1712–1723. [[CrossRef](#)]
41. Fukazawa, J.; Ohashi, Y.; Takahashi, R.; Nakai, K.; Takahashi, Y. DELLA degradation by gibberellin promotes flowering via GAF1-TPR-dependent repression of floral repressors in *Arabidopsis*. *Plant Cell* **2021**, *33*, 2258–2272. [[CrossRef](#)]
42. Sanagi, M.; Aoyama, S.; Kubo, A.; Lu, Y.; Sato, Y.; Ito, S.; Abe, M.; Mitsuda, N.; Ohme-Takagi, M.; Kiba, T.; et al. Low nitrogen conditions accelerate flowering by modulating the phosphorylation state of FLOWERING BHLH 4 in *Arabidopsis*. *Proc. Natl. Acad. Sci. USA* **2021**, *118*, e2022942118. [[CrossRef](#)] [[PubMed](#)]
43. Tayengwa, R.; Sharma, K.P.; Pierce, C.F.; Werner, B.E.; Neff, M.M. Overexpression of *AtAHL20* causes delayed flowering in *Arabidopsis* via repression of FT expression. *BMC Plant Biol.* **2020**, *20*, 559. [[CrossRef](#)] [[PubMed](#)]
44. Zhao, X.Y.; Liu, M.S.; Li, J.R.; Guan, C.M.; Zhang, X.S. The wheat TaGI1, involved in photoperiodic flowering, encodes an *Arabidopsis* GI ortholog. *Plant Mol. Biol.* **2005**, *58*, 53–64. [[CrossRef](#)] [[PubMed](#)]
45. Anwar, T.; Shehzadi, A.; Qureshi, H.; Shah, M.N.; Danish, S.; Salmen, S.H.; Ansari, M.J. Alleviation of cadmium and drought stress in wheat by improving growth and chlorophyll contents amended with GA3 enriched deashed biochar. *Sci. Rep.* **2023**, *13*, 18503. [[CrossRef](#)] [[PubMed](#)]
46. Arnon, D.I. Copper enzymes in isolated chloroplasts. Polyphenoloxidase in *Beta vulgaris*. *Plant Physiol.* **1949**, *24*, 1–15. [[CrossRef](#)] [[PubMed](#)]

47. Ahmad, I.; Zhu, G.; Zhou, G.; Liu, J.; Younas, M.U.; Zhu, Y. Melatonin role in plant growth and physiology under abiotic stress. *Int. J. Mol. Sci.* **2023**, *24*, 8759. [[CrossRef](#)] [[PubMed](#)]
48. Waadt, R.; Seller, C.A.; Hsu, P.K. Plant hormone regulation of abiotic stress responses. *Nat. Rev. Mol. Cell Biol.* **2022**, *23*, 680–694. [[CrossRef](#)]
49. Gao, Y.-F.; Liu, J.-K.; Yang, F.-M.; Zhang, G.-Y.; Wang, D.; Zhang, L.; Ou, Y.-B.; Yao, Y.-A. The WRKY transcription factor WRKY8 promotes resistance to pathogen infection and mediates drought and salt stress tolerance in *Solanum lycopersicum*. *Physiol. Plant.* **2020**, *168*, 98–117. [[CrossRef](#)] [[PubMed](#)]
50. Ampofo, J.O.; Ngadi, M. Stimulation of the phenylpropanoid pathway and antioxidant capacities by biotic and abiotic elicitation strategies in common bean (*Phaseolus vulgaris*) sprouts. *Process Biochem.* **2021**, *100*, 98–106. [[CrossRef](#)]
51. Chen, H.; Li, X.; Li, F.; Li, D.; Dong, Y.; Fan, Y. Bioinformatics analysis of wrky family genes in *Erianthus fulvus* Ness. *Genes* **2022**, *13*, 2102. [[CrossRef](#)] [[PubMed](#)]
52. Liu, Z. Identification of WRKY Transcription Factor Family in *Xanthoceras sorbifolia* and Analysis of Response Patterns to Abiotic Stresses. Master's Thesis, Northeast Forestry University, Harbin, China, 2020; p. 000390.
53. Liu, Y.X. Identification and Expression Analysis of WRKY Gene Family in Tomato. Master's Thesis, Shenyang Agricultural University, Shenyang, China, 2020; p. 000900.
54. Zhou, X.; Jiang, Y.; Yu, D. WRKY22 transcription factor mediates dark-induced leaf senescence in *Arabidopsis*. *Mol. Cells* **2011**, *31*, 303–313. [[CrossRef](#)] [[PubMed](#)]
55. Wang, Y.; Huang, X.; Huang, X.; Su, W.; Hao, Y.; Liu, H.; Chen, R.; Song, S. BcSOC1 Promotes Bolting and Stem Elongation in Flowering Chinese Cabbage. *Int. J. Mol. Sci.* **2022**, *23*, 3459. [[CrossRef](#)] [[PubMed](#)]
56. Wang, H.; Chen, W.; Xu, Z.; Chen, M.; Yu, D. Functions of WRKYs in plant growth and development. *Trends Plant Sci.* **2023**, *28*, 630–645. [[CrossRef](#)] [[PubMed](#)]
57. Long, Q.; Du, M.; Long, J.; Xie, Y.; Zhang, J.; Xu, L.; He, Y.; Li, Q.; Chen, S.; Zou, X. Transcription factor WRKY22 regulates canker susceptibility in sweet orange (*Citrus sinensis* Osbeck) by enhancing cell enlargement and CsLOB1 expression. *Hortic. Res.* **2021**, *8*, 50. [[CrossRef](#)] [[PubMed](#)]
58. Wu, Z.; Li, T.; Cao, X.; Zhang, D.; Teng, N. Lily WRKY factor LIWRKY22 promotes thermotolerance through autoactivation and activation of *Lldreb2b*. *Hortic. Res.* **2022**, *9*, uhac186. [[CrossRef](#)] [[PubMed](#)]
59. Zhao, S. Identification of WRKY gene family in chestnut and analysis of its expression under drought stress. *North China J. Agron.* **2024**, *39*, 72–82.
60. Balti, I.; Benny, J.; Perrone, A.; Caruso, T.; Abdallah, D.; Salhi-Hannachi, A.; Martinelli, F. Identification of conserved genes linked to responses to abiotic stresses in leaves among different plant species. *Funct. Plant Biol.* **2020**, *48*, 54–71. [[CrossRef](#)] [[PubMed](#)]
61. Li, Y.; Han, S.; Sun, X.; Khan, N.U.; Zhong, Q.; Zhang, Z.; Zhang, H.; Ming, F.; Li, Z.; Li, J. Variations in *OsSPL10* confer drought tolerance by directly regulating *OsNAC2* expression and ROS production in rice. *J. Integr. Plant Biol.* **2023**, *65*, 918–933. [[CrossRef](#)] [[PubMed](#)]
62. Anuradha, M.; Sivaraju, K.; Krishnamurthy, V. Effect of waterlogging on physiological characteristics, yield and quality of flue-cured tobacco. *Indian J. Plant Physiol.* **2013**, *18*, 67–70. [[CrossRef](#)]
63. Elshoky, H.A.; Yotsova, E.; Farghali, M.A.; Farroh, K.Y.; El-Sayed, K.; Elzorkany, H.E.; Rashkov, G.; Dobrikova, A.; Borisova, P.; Stefanov, M.; et al. Impact of foliar spray of zinc oxide nanoparticles on the photosynthesis of *Pisum sativum* L. under salt stress. *Plant Physiol. Biochem.* **2021**, *167*, 607–618. [[CrossRef](#)]
64. Razi, K.; Muneer, S. Drought stress-induced physiological mechanisms, signaling pathways and molecular response of chloroplasts in common vegetable crops. *Crit. Rev. Biotechnol.* **2021**, *41*, 669–691. [[CrossRef](#)] [[PubMed](#)]
65. Zahra, N.; Al, H.M.; Hafeez, M.B.; Rehman, A.; Wahid, A.; Siddique, K.; Farooq, M. Regulation of photosynthesis under salt stress and associated tolerance mechanisms. *Plant Physiol. Biochem.* **2022**, *178*, 55–69. [[CrossRef](#)] [[PubMed](#)]
66. Gill, S.S.; Tuteja, N. Reactive oxygen species and antioxidant machinery in abiotic stress tolerance in crop plants. *Plant Physiol. Biochem.* **2010**, *48*, 909–930. [[CrossRef](#)]
67. Skopelitis, D.S.; Paranychianakis, N.V.; Paschalidis, K.A.; Pliakonis, E.D.; Delis, I.D.; Yakoumakis, D.I.; Kouvarakis, A.; Papadakis, A.K.; Stephanou, E.G.; Roubelakis-Angelakis, K.A. Abiotic stress generates ROS that signal expression of anionic glutamate dehydrogenases to form glutamate for proline synthesis in tobacco and grapevine. *Plant Cell* **2006**, *18*, 2767–2781. [[CrossRef](#)]
68. Jaleel, C.A.; Riadh, K.; Gopi, R.; Manivannan, P.; Inès, J.; Al-Juburi, H.J.; Chang-Xing, Z.; Hong-Bo, S.; Panneerselvam, R. Antioxidant defense responses: Physiological plasticity in higher plants under abiotic constraints. *Acta Physiol. Plant* **2009**, *31*, 427–436. [[CrossRef](#)]
69. Blumwald, E. Sodium transport and salt tolerance in plants. *Curr. Opin. Cell Biol.* **2000**, *12*, 431–434. [[CrossRef](#)] [[PubMed](#)]
70. Moriau, L.; Bogaerts, P.; Jonniaux, J.L.; Boutry, M. Identification and characterization of a second plasma membrane H⁽⁺⁾-ATPase gene subfamily in *Nicotiana plumbaginifolia*. *Plant Mol. Biol.* **1993**, *21*, 955–963. [[CrossRef](#)]
71. Qin, L.J.; Song, L.L.; Zhao, D.; Zhao, D.G. Overexpression of tobacco high-affinity potassium High affinity kalium transporter1 gene (*NtHAK1*) increased tobacco salt stress ability. *J. Agric. Biotechnol.* **2015**, *23*, 1576–1587.

Disclaimer/Publisher's Note: The statements, opinions and data contained in all publications are solely those of the individual author(s) and contributor(s) and not of MDPI and/or the editor(s). MDPI and/or the editor(s) disclaim responsibility for any injury to people or property resulting from any ideas, methods, instructions or products referred to in the content.